Research Square

Preprints are preliminary reports that have not undergone peer review.
They should not be considered conclusive, used to inform clinical practice,
or referenced by the media as validated information.

Temperature-Induced Displacement Behavior of a Hybrid Cable-Stayed and Suspension Bridge Based on Long-Term Field Monitoring

Biehn Baik

vinie99@hotmail.com

WSP Canada Inc

Research Article

Keywords: Yavuz Sultan Selim Bridge, bridge, SHMS, temperature, thermal effect, displacement

Posted Date: November 11th, 2026

DOI: https://doi.org/10.21203/rs.3.rs-11668393/v1

License: This work is licensed under a Creative Commons Attribution 4.0 International License.
Read Full License

Additional Declarations: The authors declare no competing interests.

Temperature-Induced Displacement Behavior of a Hybrid Cable-Stayed and Suspension Bridge Based on Long-Term Field Monitoring

Biehn Baik[1], Ahmet Kaan Akpunar[2]

Abstract

Temperature-induced deformation is a dominant component of the long-term response of long-span bridges, yet its behavior under in-service conditions remains insufficiently quantified, particularly for hybrid structural systems. This study investigates the temperature distribution and temperature-induced displacement behavior of the Yavuz Sultan Selim Bridge in Türkiye, a combined cable-stayed and suspension bridge with mixed steel and concrete deck systems, using long-term field measurements supported by numerical analysis. Temperature and displacement data recorded by the bridge's permanent Structural Health Monitoring System, in continuous operation since 2016, are analyzed to evaluate daily and seasonal thermal effects. Measured deck temperatures are decomposed into effective uniform temperature and sectional temperature gradients, and their relationships with longitudinal and vertical displacements at abutments, tower bearings, and midspan are examined. The results show strong linear correlations between effective deck temperature and longitudinal displacements at supports, while vertical displacements are interpreted as secondary responses associated with longitudinal thermal expansion. At midspan, seasonal temperature variation governs vertical deck displacement, with measured amplitudes comparable to design-stage analytical predictions.

Keywords: Yavuz Sultan Selim Bridge; bridge; SHMS; temperature; thermal effect; displacement.

1. Introduction

Monitoring the dynamic behavior of long-span bridges is critical for ensuring structural durability and safety. Among various environmental factors, thermal actions play a significant role in influencing bridge performance. Bridges experience daily and seasonal temperature variations due to solar radiation and ambient air temperature changes. These fluctuations induce complex structural responses, affecting geometry, mechanical properties, and boundary conditions. Accurately quantifying these effects remains a challenge due to their nonlinear and time-dependent characteristics. Several studies have suggested that environmental thermal effects might have a greater impact on structural behavior

[1] Technical Lead, Bridges Dept., WSP Global Inc., Mississauga, ON, Canada L5N 7K2 (former Bridge Engineer, Chodai Co., Ltd., Tokyo, Japan). Email: biehn.baik@wsp.com

[2] Project Executive, Project Investment Dept., Akcansa-Heidelberg Cement JV, Istanbul, Türkiye 34535 (former Bridge Engineer, Yüksel Proje, Ankara, Türkiye). ORCID: https://orcid.org/0000-0002-5636-6613. Email: ahmetkaanakpunar@hotmail.com

than external operational loads, potentially leading to unexpected deformations, fatigue, and long-term damage.

Previous studies have investigated thermal effects on various bridge types, developing numerical models, field monitoring, or a combination of them.

Lan et al. [3] developed an improved numerical model for analyzing wind-induced thermal effects on a box-girder bridge, using hourly simulations. Their study demonstrated the importance of considering wind in thermal analysis, relying primarily on numerical simulations.

Linren et al. [4] investigated the temperature behavior of a long-span suspension bridge using approaches of field monitoring and numerical analysis. The study analyzed both vertical and transversal temperature differences and validated temperature distribution models for the Humber Bridge. Their analysis was based on a 24-hour dataset, capturing only short-term fluctuations without assessing seasonal and long-term thermal effects. They acknowledged the need for future studies to acquire temperature data over an extended period in an in-service bridge, allowing for a more comprehensive understanding of long-term temperature distributions and their impact on structural behavior.

Xia et al. [5] and Xu et al. [2] investigated temperature behavior of the Tsing Ma Suspension Bridge, integrating numerical simulations and field monitoring data. Their analysis relied on temperature and displacement data collected for a single day (July 17, 2005) with hourly variations, providing understanding of short-term hourly fluctuations. However, long-term seasonal variations and cumulative thermal effects are essential for understanding temperature-induced movements over extended periods. These long-term thermal effects may play a crucial role in structural performance, fatigue assessment, and potential damage accumulation.

Lucas et al. [7] analyzed the thermal effects in the orthotropic box girder and in stay cables of the Normandy Bridge. They analyzed the average temperature and thermal gradient of a steel box-girder bridge, which showed that a steel box-girder bridge would have a large temperature gradient along the cross section and significant variation over time. For practical purposes, they compared the calculated results with the measured values to justify the numerical model, but actual structural movements caused by these thermal effects were not considered.

Shashi et al. [11] developed a theoretical method of predicting bridge temperatures and the resulting movements for skewed and curved bridges. They highlighted discrepancies between AASHTO temperature assumptions and actual conditions and then verified their analytical model by comparing with a short-term (3-day) field test data.

This study aims to investigate the long-term thermal behavior of a hybrid long-span bridge using one year of field monitoring data (December 2016 – November 2017). By analyzing seasonal variations and cumulative thermal effects, this research provides a comprehensive assessment of temperature-induced displacements over an extended period. Additionally, the measured

displacements are compared with calculated values from the design phase, enabling validation of thermal movement assumptions and improving predictive accuracy for future bridge designs.

2. Bridge and Structural Health Monitoring System

2.1. Bridge System

The Yavuz Sultan Selim (YSS) Bridge, located in Türkiye, is a hybrid long-span bridge that combines cable-stayed and suspension systems within a single structural configuration. With a total length of 2,164 m, the bridge consists of a central main span of 1,408 m and two side spans of 378 m each. This hybrid structural arrangement results in a complex load-transfer mechanism and global stiffness characteristics that differ from those of conventional suspension or cable-stayed bridges.

The bridge deck system varies along the longitudinal direction. An orthotropic steel box girder is employed in the main span, while prestressed concrete box girders are used in the side spans [1]. The coexistence of steel and concrete decks introduces distinct thermal expansion characteristics along the bridge length, making the structure particularly sensitive to temperature variation and thermal gradients.

Boundary conditions further contribute to the complexity of the bridge's thermal response. The deck is supported by tower bearings and abutment bearings with different restraint conditions, including fixed and longitudinally movable supports, as well as expansion joints at the abutments. These constraints govern how thermal expansion and contraction are redistributed along the bridge and directly influence displacement patterns at critical locations.

Due to its exceptional span length, mixed deck materials, and hybrid structural system, thermal actions play a dominant role in governing the global deformation behavior of the YSS Bridge. As a result, accurate characterization of temperature-induced displacement is essential for understanding its in-service structural performance.

2.2. Structural Health Monitoring System Application

To monitor the in-service behavior of the Yavuz Sultan Selim Bridge and to capture its response to environmental actions, a permanent Structural Health Monitoring (SHM) system was installed and has been in continuous operation since the bridge opened to traffic in 2016. The primary objective of the SHM system is to record long-term structural response data under actual operational and environmental conditions.

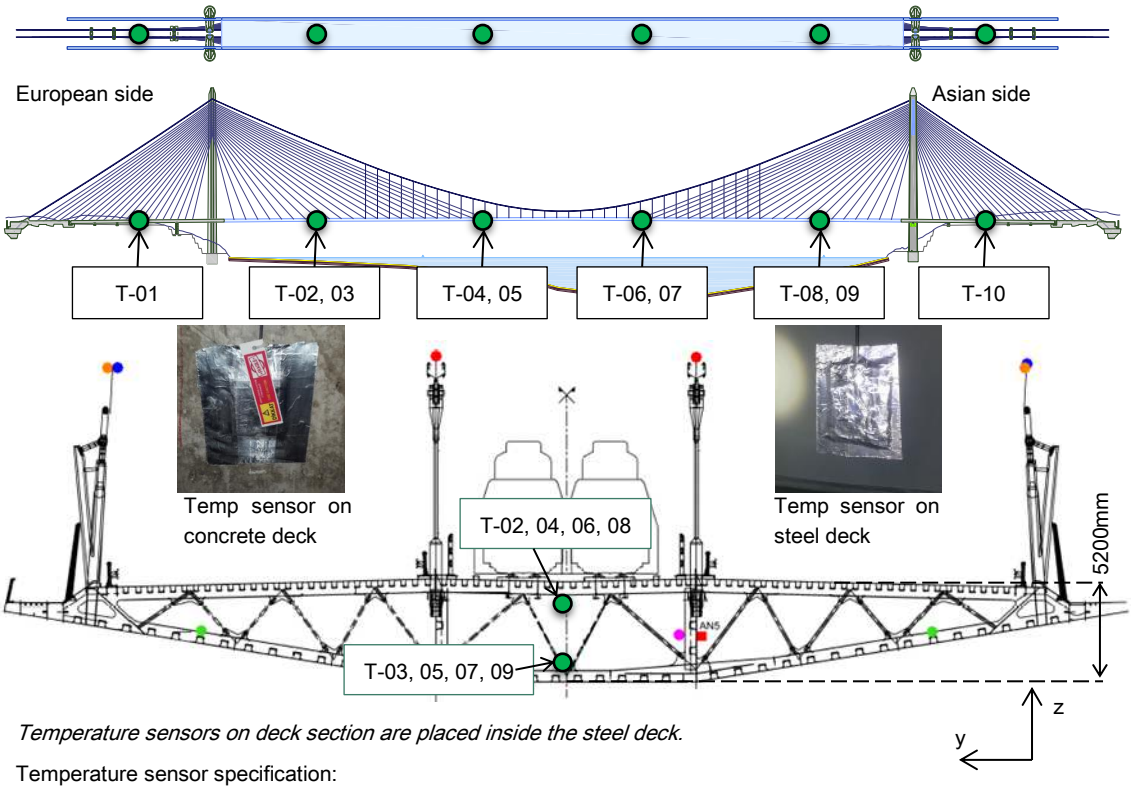
An important advantage of continuous monitoring is that it provides information on the condition and configuration of the structure in real time, such that any changes (e.g., sudden changes due to an extreme event such as an earthquake, or slow changes due to environmental factors, aging, and deterioration) can be detected and identified immediately [2].

In the present study, temperature and displacement measurements obtained from the SHM system are used to investigate temperature-induced structural behavior.

2.3. Temperature Sensor Network

Temperature sensors are installed at representative locations within both the steel and concrete deck sections, allowing measurement of deck section temperatures as well as ambient air temperature. Their positions are shown in **Figure 1** in which the numbers in boxes are the sensor identification numbers at the different positions.

The collected temperature data from the SHMS can be grouped into three categories: (1) air temperature (TH-1, set on the control room); (2) concrete deck section temperature (T-01, 10); and (3) steel deck section temperature (T-02 to T-09). An air temperature sensor (TH-1) is at the outside roof of the control room where the SHMS is in operation. Two temperature sensors (T-01, T-10) are placed at the middle sections of concrete box decks in the European- and the Asian-side back spans. And other 8 temperature sensors are placed on the upper and the lower decks inside an orthotropic steel deck and measuring the deck section temperature of the main span. The SHMS is providing these temperature data daily in the 10-minute sampling rate.



Temperature sensors on deck section are placed inside the steel deck.

Temperature sensor specification:

- Type: J type
- Surface mountable
- Operating temperature range: -60 to +120℃
- Error limit: < 1.0 ℃

Figure 1 Position of temperature sensors and cross section of the YSS Bridge

2.4. Displacement Sensor Network

Displacement sensors are installed at critical structural interfaces, including abutments and tower bearings, to measure longitudinal and vertical movements of the bridge deck. These locations were selected because thermal expansion and contraction are expected to demonstrate most clearly at supports and expansion joints. The displacement sensors measure relative movement between fixed and movable structural components, enabling evaluation of temperature-related deformation over time.

The positions of displacement sensors on the European side of the YSS Bridge are shown in **Figure 2** in which the numbers in boxes are the sensor identification numbers at different positions. It goes in the same way on the opposite Asian side.

Displacement sensors can measure the length modification between a fixed part and a movable one. They will be used to monitor bearing movement and expansion joint movement. The sensor type and its installation are shown in **Figure 3**. Using steel or aluminum structure, sensors were placed to monitor the vertical and the longitudinal movement of the deck depending on their locations. At expansion joint, sensors were placed under the deck, each edge of the sensor fixed to each side of the joint. Sensors were installed parallel to the bridge.

The collected data from these displacement sensors are stored in the form of the wire length of each displacement sensor, so each wire length can be different depending on the sensor configuration at each position.

For monitoring displacement variation with respect to one-year term temperature change, two locations are picked up where are abutments (D-01, 02) and tower bearings (D-10, 11) and their displacement data are calculated as the daily average displacements. And these displacements are plotted and compared to the effective temperature.

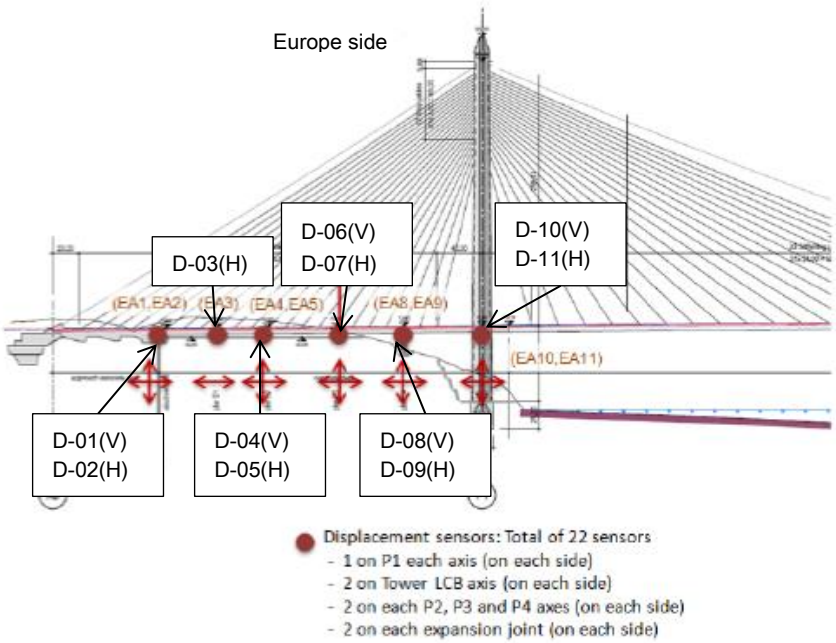


Figure 2 Locations of displacement sensors on the European side of the YSS Bridge

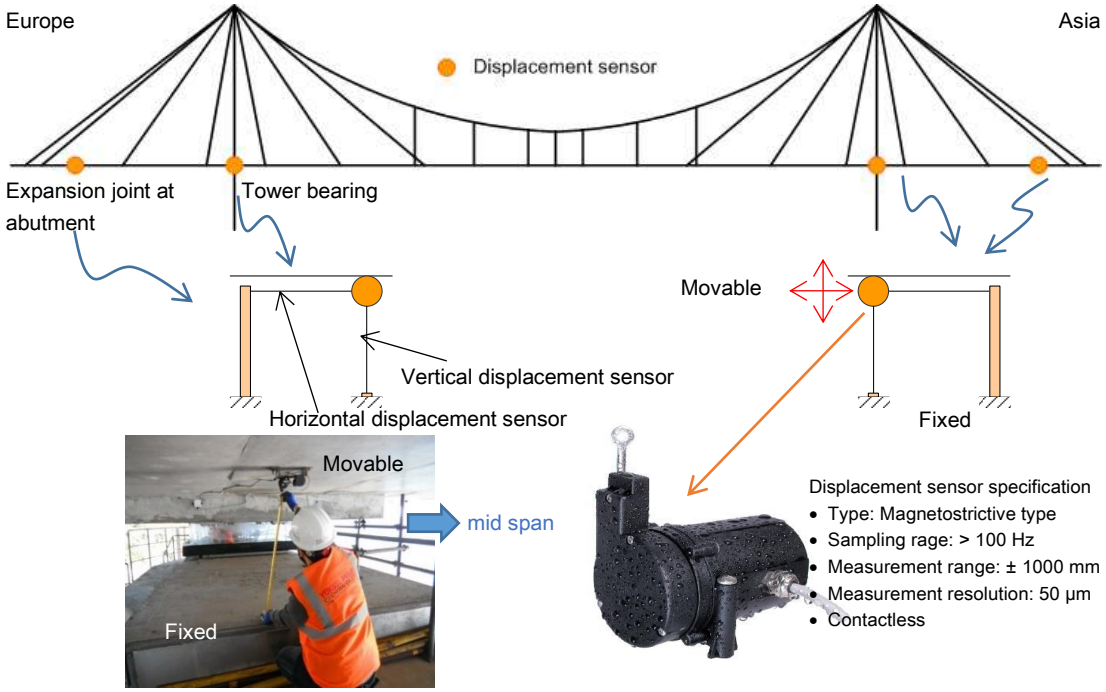
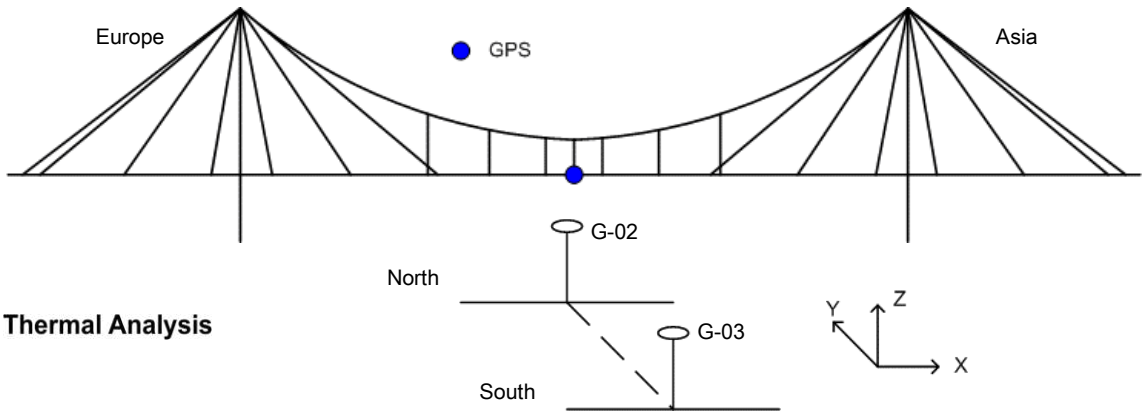


Figure 3 Displacement sensor type and installation

For the displacements of the bridge deck, it is noted that the displacements are obtained from where two GPS stations were installed on the bridge deck (**Figure 4**).



3. Thermal Analysis

Figure 4 Position of GPS sensors on bridge deck

To evaluate temperature-induced structural response, the measured temperature field of the bridge deck is decomposed into representative thermal components that can be directly related to

global deformation behavior. In accordance with established practice for long-span bridges, the thermal field is expressed as a combination of a uniform effective temperature and sectional temperature gradients. This decomposition enables separation of global expansion effects from local bending effects and provides a consistent basis for interpreting temperature-induced displacement.

3.1. Temperature Calculation

With respect to given time, temperature field over the cross section (**Figure 1**) varies and should be considered. A two-dimensional temperature field on the cross section is usually decomposed into a uniform part T_{eff}, called the average effective temperature, two linear gradients GT_y and GT_z, as described in the following equations [6]:

$$T_{eff} = \frac{1}{A}\iint_A T(y,z)dy\,dz \tag{1}$$

$$GT_y = \frac{1}{I_z}\iint_A T(y,z)ydA \tag{2}$$

$$GT_z = \frac{1}{I_y}\iint_A T(y,z)zdA \tag{3}$$

where A is the cross-sectional area of the steel deck, and I_y and I_z the moment of inertia of the steel deck cross section with respect to the y and z axes, respectively.

3.2. Thermal Action Assessment

From these equations, the daily average effective temperature in x-axis can be calculated and two temperature gradients in the y and z axes are estimated.

In addition to these thermal component equations, to consider thermal actions on bridge deck, Eurocode 1 [6] suggests:

- Representative values of thermal actions should be assessed by the uniform temperature component and the temperature difference components.
- The uniform temperature component depends on the minimum and maximum temperature which a bridge will achieve.
- And the values of minimum and maximum shade air temperatures for the site location shall be obtained, and based on them, the variation of the temperatures which a bridge will receive should be assessed.
- Then these values affect heating and cooling of a bridge deck's upper surface that will result in a maximum heating (top surface warmer) and a maximum cooling (bottom surface warmer) temperature variation.

In this study, the Eurocode-based framework is used not as a prescriptive design check, but as a reference model against which measured temperature distributions are evaluated. This allows direct comparison between design assumptions and actual in-service thermal behavior.

As the number of sensors was limited and measurement was taken at discrete points, we have assumed that temperatures are constant in the vicinity of sensors and each temperature sensor on the upper and the lower decks represents temperature distribution on each individual steel plate of a cross section [6]. Furthermore, it has been studied that temperature differences in the longitudinal direction of a bridge are generally neglected [8]. Therefore, all of temperature sensors on the main span represent in the assessment of the average temperature in the steel deck cross section. With the measured data on the upper and the lower decks, the temperature distribution on the orthotropic steel deck cross section is evaluated.

A limited number of temperature records exhibiting abnormal values outside historical climatic ranges were excluded from the analysis. These outliers are attributed to sensor malfunction or data acquisition issues. Their exclusion does not affect the observed seasonal trends or the linear relationships identified in subsequent analyses, as the evaluation focuses on long-term average behavior rather than isolated extreme events.

Based on the characterized effective temperature and sectional gradients, the resulting thermal actions provide a rational basis for interpreting measured displacement behavior and for assessing temperature-induced deformation mechanisms, which are examined in the following sections.

4. Temperature Behavior of the YSS Bridge

4.1. Temperature Distribution

As of the end of 2017, it had been almost a year since the SHMS started recording the measurement data on 1 Dec 2016, temperature variations for a year were obtained.

It is common on the surface of the deck that daily temperatures vary the most. The biggest range observed during a day was about 37℃ on the 30/06/2016 between the day temperature of 57℃ and the night temperature of 20℃ from T-04.

For monitoring one-year term temperature variation, with temperature data obtained from eight temperature sensors (T-02~09) on the main span, deck effective temperature is defined and calculated as daily average temperatures of four locations within steel deck cross section.

And these temperatures are considered measuring ambient temperatures around the steel deck section. In addition, air temperature data obtained from the air temperature sensor (TH-1) are calculated as daily average air temperature and then compared to the deck effective temperature defined above, as shown in **Figure 5**.

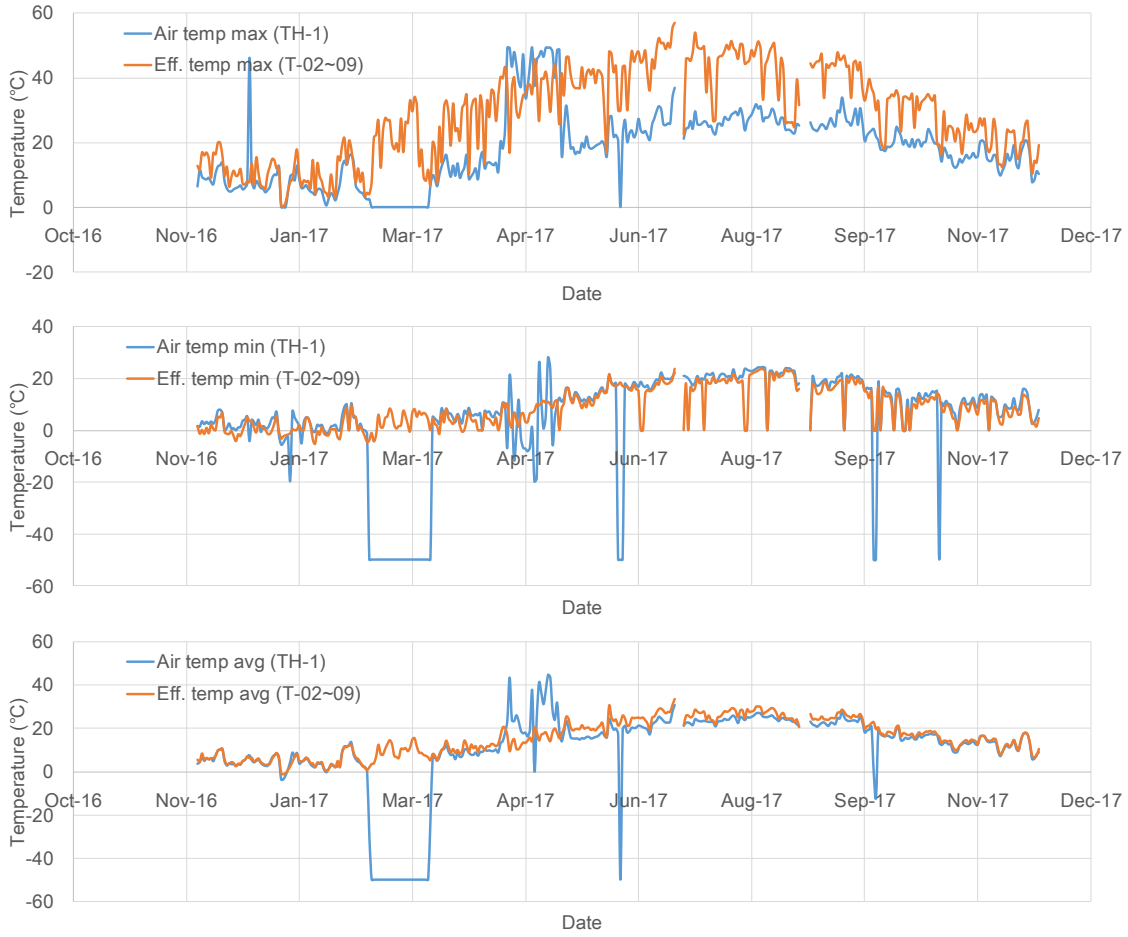
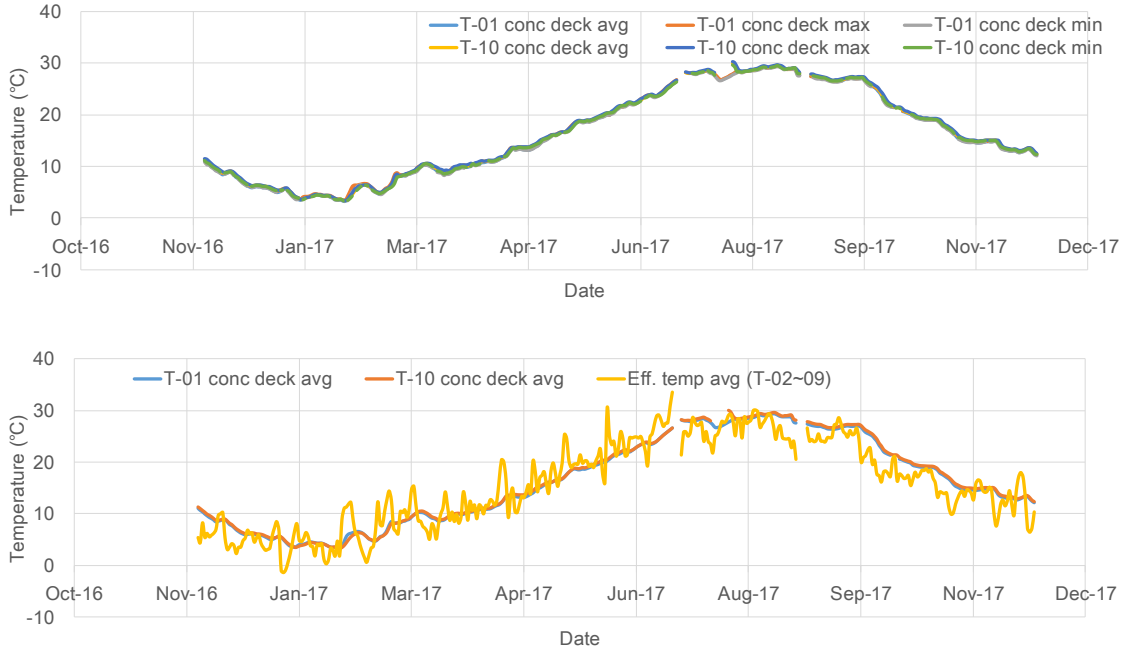


Figure 5 Daily max, min, and average air temperatures, and deck effective temperatures during 01/12/2016 to 30/11/2017

As a result, some data missing or drifting extremely out of overall trends are seen and a few of them are out of the range of -11.7 to 41.5, which are the minimum and maximum recorded air temperatures (on a period of 52 years and for two meteorological stations located close to the bridge) [9]. These might be caused by a malfunction occurring in some sensors or there might be something failure near them or near data acquisition units. Such abnormal components of the data are excluded from thermal effect evaluation. As considered as a whole, the average air temperature for a year resulted in 15.1°C, equal to the bridge reference temperature, 15°C, assumed and adopted at the design phase.

Deck temperature data measured on two temperature sensors (T-01, T-10) on concrete decks are plotted and compared to the deck effective temperature data, as shown in **Figure 6**. As a result, less differences are seen between daily maximum, minimum, and average values of T-01 and T-10. And from comparison made of these daily average temperatures with those of the deck effective

238 temperatures, they are well matched. Therefore, it can be assumed that the deck effective temperatures
239 represent long-term structural temperatures.
240



241
242 Figure 6 Daily max, min, and average temperatures on concrete deck, and deck effective
2434.2. temperatures
244

245 ## Analysis of Daily Cycles

246 For the summer season, the temperature in the upper deck plate is much higher than the ambient
247 air one during the afternoon. The difference can reach 21.5℃ (49.3-27.8). The average deck
248 temperature (from 8 points) is also higher than the ambient one by 10.3℃ (38.1-27.8) on the same day
249 (July 30, 2017), as shown in **Figure 7.**

250 The solar radiation normally gives much impact on the deck's temperature change, but the present
251 monitoring system does not consist of any component to enable to measure such a degree of solar
252 radiation to which the steel deck exposes itself.

253 In order to figure out the relationship between vertical thermal gradient and solar radiation, the
254 past solar radiation data, the average hourly solar radiation in Istanbul measured in July and January
255 from1992 to 1993 [9], are employed.

256 The vertical thermal gradient reaches 22℃ and it follows at the peak of the average hourly solar
257 radiation in July, which indicates the high gradient is affected much by the solar radiation.

258 For the winter season, the average temperature of the deck plate corresponds roughly with the
259 ambient air temperature. The vertical thermal gradient reaches 1℃ at the peak of the average hourly

solar radiation in January, as shown in **Figure 8**. This leads to small solar radiation that may cause less thermal effect to the steel deck.

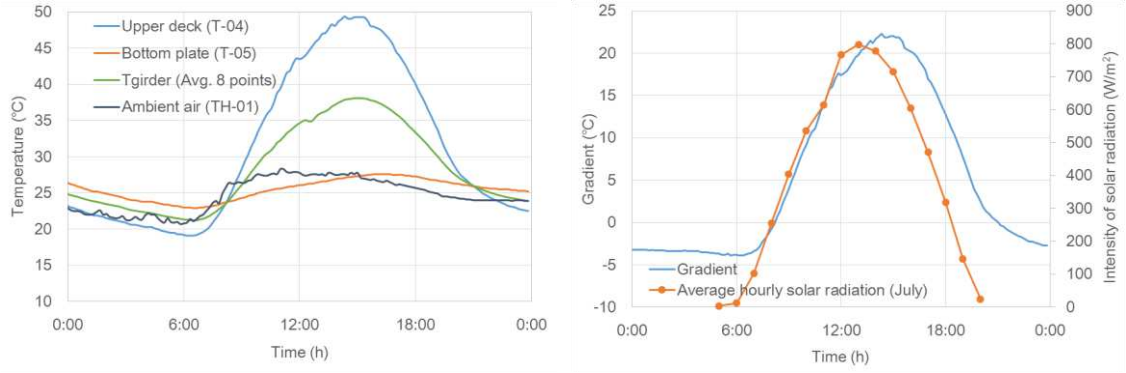


Figure 7 Temperatures in the steel deck on July 30, 2017

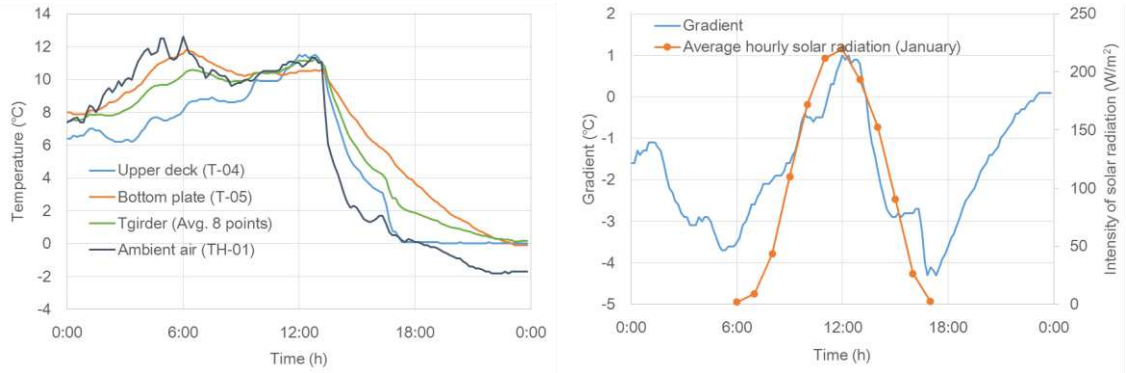


Figure 8 Temperatures in the steel deck on January 6, 2017

4.3.

4.3.1.

Extreme Temperature Distribution

Maximum Effective Temperature

A direct correlation between the daily maximum effective temperature in the steel deck and the daily ambient air temperature recorded during the monitoring period is investigated. (**Figure 9**). The correlation described in Eurocode 1 is also plotted together and most of the high measured values are

4.3.2. somewhat over the baseline of Eurocode 1.

The maximum effective temperature in the steel deck (57°C on June 30, 2017) is much higher than the ambient air temperature (37°C on June 30, 2017), and the maximum daily difference, $(T_{eff} - T_{air})_{max}$ which is equal to 26°C in **Figure 9**.

Minimum Effective Temperature

A direct correlation between the daily minimum effective temperature in the steel deck and the daily ambient air temperature recorded during the monitoring period is investigated. (**Figure 10**). The correlation described in Eurocode 1 is also plotted together.

The minimum effective temperature in the steel deck (-3.2℃ on January 7, 2017) is a little higher than the ambient air temperature (-5.5℃ on January 7, 2017). The daily difference, $(T_{eff} - T_{air})_{min}$, is equal to -2.3℃. This result agrees with the baseline given in Eurocode 1.

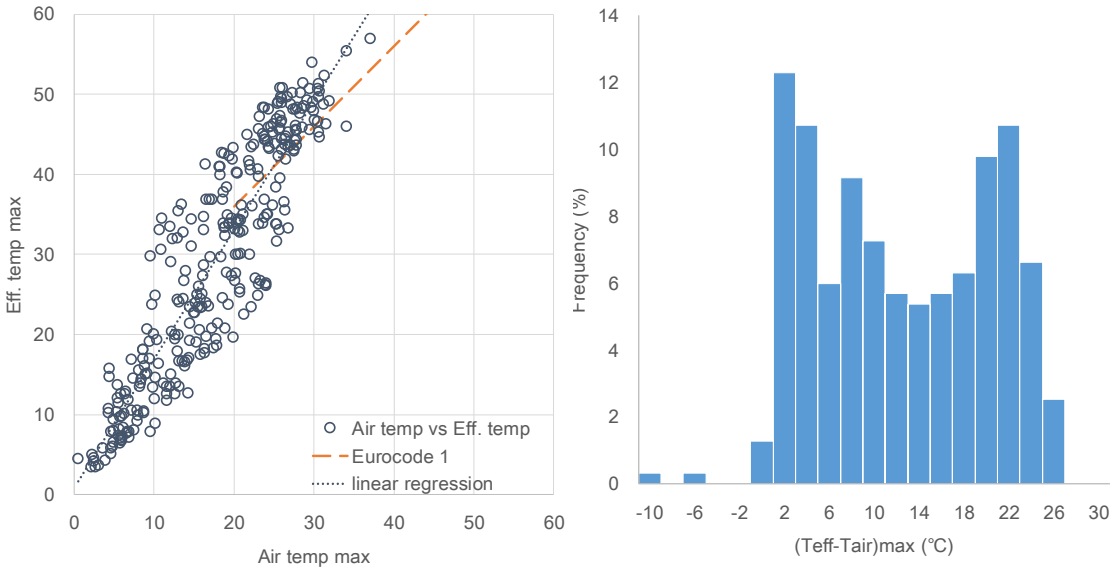


Figure 9 (a) Daily maximum effective temperature versus ambient air temperature, and (b) Distribution of maximum differences between maximum effective temperature and ambient air temperature (Dec 2016 to Nov 2017)

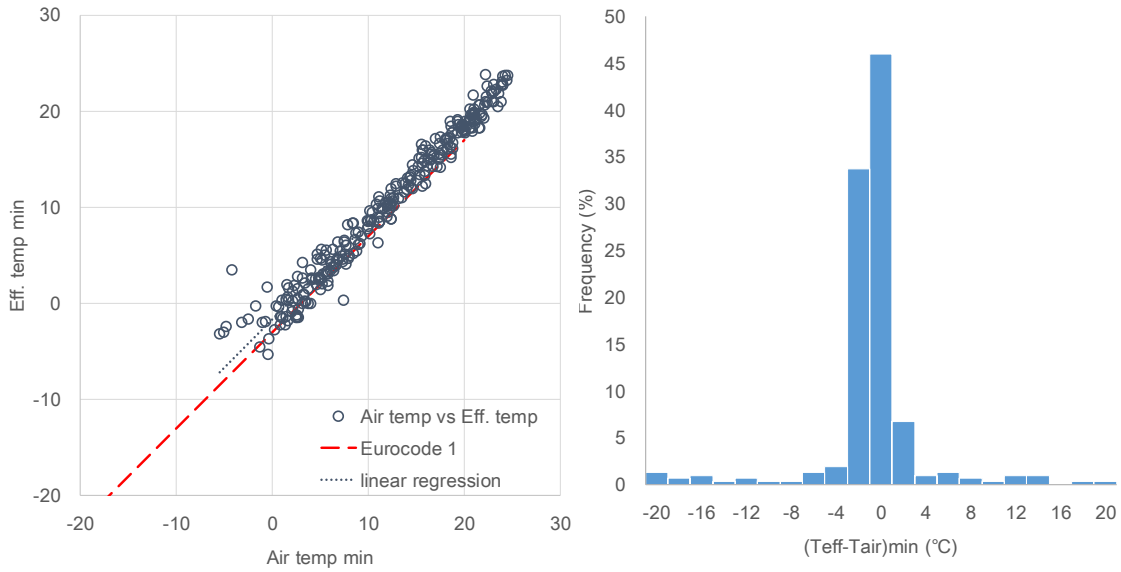


Figure 10 (a) Daily minimum effective temperature versus ambient air temperature, and (b) Distribution of maximum differences between minimum effective temperature and ambient air temperature (Dec. 2016 to Nov. 2017)

4.4. Extreme Temperature Vertical Gradient

4.4.1. Maximum Vertical Gradient

As the daily maximum effective temperatures increase, the vertical gradients become large. **Figure 11** shows the correlation between the daily maximum effective temperature on the *x*-axis and the maximum vertical gradient on the *y*-axis. It appears that the data are scattered but the correlation looks linear, which can be expressed as:

$$GT_{z\,max} = 0.5T_{eff\,max} - 2.6 \quad (4)$$

4.4.2. Minimum Vertical Gradient

The minimum gradient measured is -6°C low, measured in the winter, as shown in **Figure 11**. The value is higher than -13°C, the recommended value for steel deck in the case of bottom warmer than top in Eurocode 1.

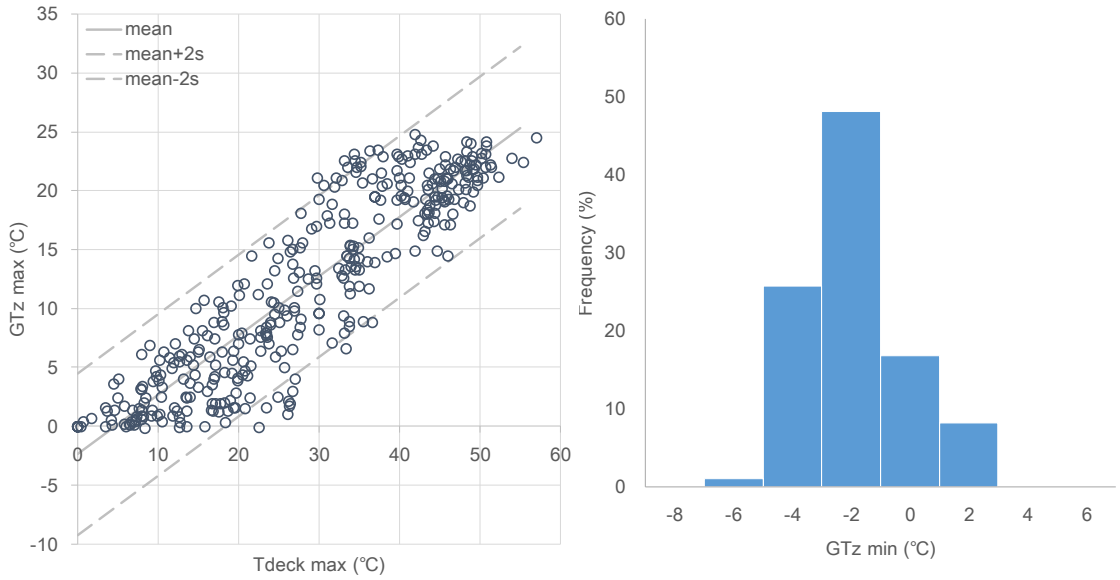


Figure 11 (a) Daily maximum effective temperature and of the vertical gradient, and (b) Distribution of minimum daily vertical gradient

4.5. Numerical Analysis for Temperature-induced Displacement

Long-term thermal actions normally affect the entire bridge structure, which shows its response in the form of displacement, strain, and stress.

At design stage, the critical impact caused by thermal actions should be figured out to determine threshold values of such structural phenomena and the values will be taken as technical criteria for operation and maintenance later. Therefore, for a service life, static analysis with temperature loading cases defined was carried out and their results were presented [10]. In the analysis, loading cases corresponding to thermal effects on steel and concrete decks are shown in **Table 1**.

Table 1 Temperature loading cases for numerical analysis (Unit: Celsius)

Cases	ΔT Steel deck	ΔT Concrete deck	Vertical gradient steel deck	Vertical gradient concrete deck	Transverse gradient steel deck	Transverse gradient concrete deck
1	46	30	16	12	3	0
2	46	30	16	12	-3	0
3	37	30	20	0	3	0
4	37	30	20	0	-3	0
5	-30	-30	-5	-3	0	0
6	-30	-25	-5	-3	0	0

A global 3D beam model was developed, and the global axes system consisted of *x*-axis in longitudinal direction with *x*=0 at the center of the bridge; *y*-axis in transverse direction with *y*=0 at

symmetry plane; and *z*-axis in vertical direction with *z*=0 at sea level, respectively. As a result, support displacements at deck level were calculated in Table **2**.

Table 2 Calculated displacements at supports

	Unit	Dx min	Dx max
Abutment (Europe)	m	-0.279	0.385
Tower bearing P1 (Europe)	m	-0.186	0.285
Tower bearing P2 (Asia)	m	-0.286	0.187
Abutment (Asia)	m	-0.383	0.278

The displacement values of steel deck at mid-span are given in Table **3**.

Table 3 Calculated displacements at mid-span

Direction	Unit	Min	Max
Longitudinal (x)	m	-0.387	0.387
Transverse (y)	m	-0.008	0.008
Vertical (z)	m	-0.744	0.827

The seasonal temperature-induced bridge displacements for a year can be obtained from data measured by the monitoring system. These numerical results are compared to and evaluate the measured displacement data.

5. Temperature-induced Displacement from Field Measurements

5.1. Displacement Behavior at Bridge Abutment

It is commonly expected that the displacement in the longitudinal direction increases along with the seasonal transition from the winter to the summer.

As can be seen in **Figure 12**, the wire length of the horizontal displacement sensor is getting shorter ($L_{h0} > L_{h1}$) when the bridge deck becomes to elongate from mid span to abutment in the longitudinal direction when the deck effective temperature increases.

In addition, these days the wires of the vertical displacement sensors have been found inclined to some extents toward the back span. In the same way, when the bridge deck span moves from A_0 to A_1, the inclined wire length of the vertical displacement sensor is getting longer ($L_{v0} < L_{v1}$). For this reason, the observed vertical displacements are interpreted as secondary responses associated with longitudinal displacement of the bridge deck.

It is assumed that the lengths of the wires of the displacements on 1 Dec 2016 would have the initial values of the associated displacement record, which means the measurement starts on a given shape of the structure.

The daily calculations of longitudinal displacement of the European- and the Asian-side abutments are drawn in **Figure 13** as compared with each other recorded, showing a good agreement.

The displacements calculated in the longitudinal direction (*x*-axis) are obviously correlated with the seasonal variation and reach approximately 200 mm relative to the initial winter reference state in the summer.

The wire lengths of the vertical displacement sensors on 1 Dec 2016 were recorded 1,009 mm at the European side abutment, and 465 mm at the Asian side abutment, assumed as the initial values set on the starting point. Accordingly, all reported displacements represent relative variations with respect to the initial monitored configuration rather than absolute structural positions.

As can be seen in **Figure 14**, the vertical displacements are likewise expected to show minor increases and decreases in a back-and-forth pattern associated with the seasonal transition from winter to summer.

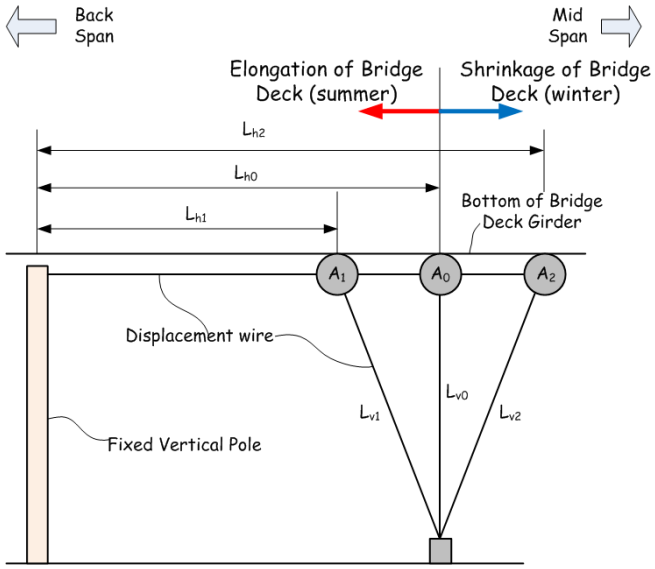


Figure 12 Displacement sensor movement with the seasonal transition

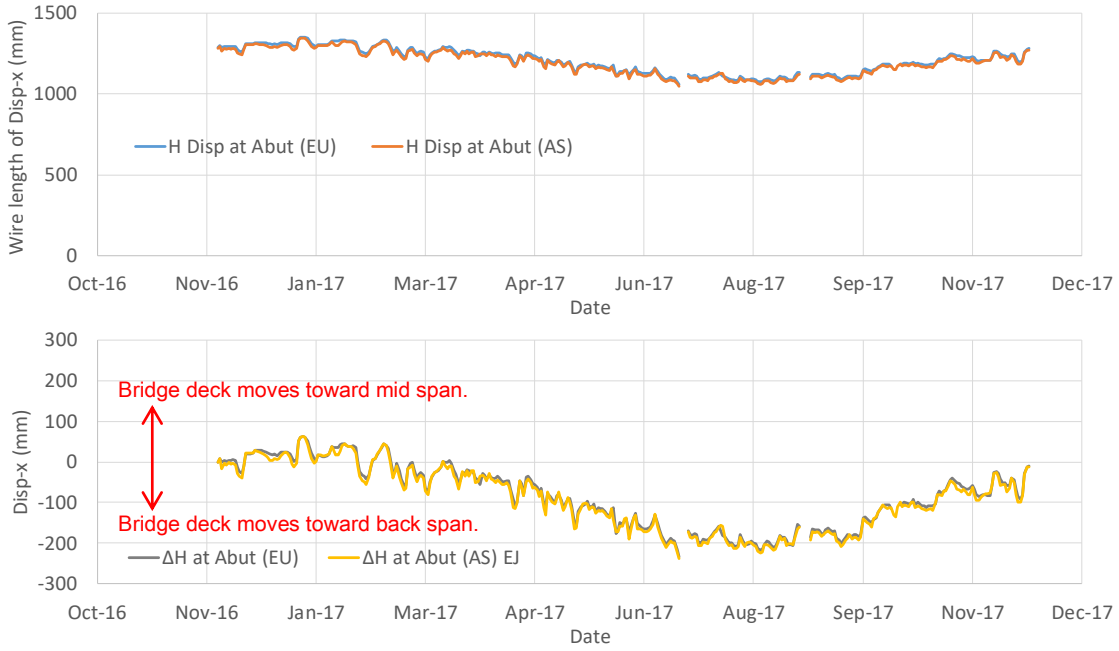


Figure 13 Daily average displacement at bridge abutment in the longitudinal direction

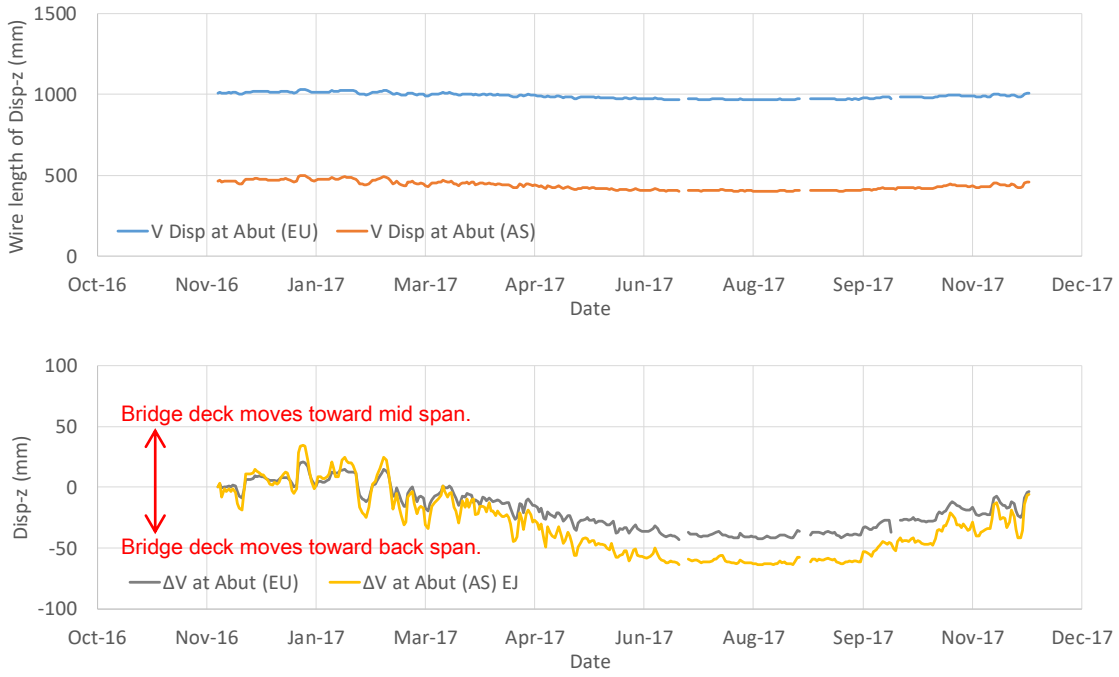
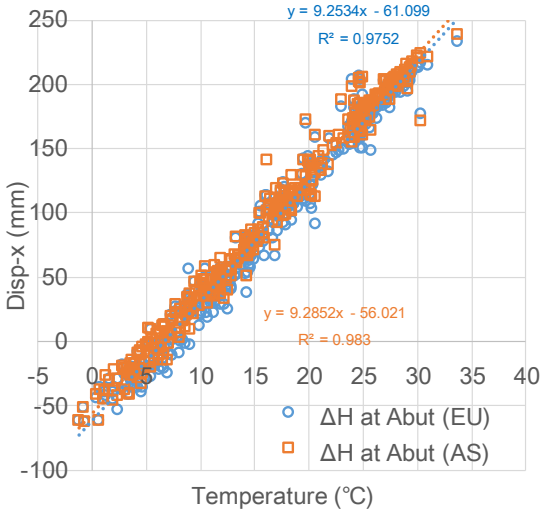


Figure 14 Daily average displacements at bridge abutments in the vertical direction

The daily average displacements of the bridge abutments in the longitudinal direction during Dec 2016 to Nov 2017 are plotted with respect to the deck effective temperature for exploring the temperature-displacement relationship, as shown in **Figure 15**.

382 The measured values are within the range of the maximum and the minimum values obtained
383 from the numerical analysis.
384



385

386 Figure 15 Relationship between daily average longitudinal displacements at bridge abutments and
387 deck effective temperature
388

389 The daily longitudinal displacements present a very good linear relationship with the deck
390 effective temperature. The corresponding linear regression model is taken as

391 $$y = at + b + \varepsilon_y \quad [5]$$

392 where y is the displacement, a (slope) and b (intercept) are regression coefficients, and ε_y is the
393 error. With least-square fitting, the regression coefficients are obtained as a = 9.253 mm/°C and b = -
394 61.099 mm for the longitudinal displacement in the abutment (Europe), and a = 9.285 mm/°C and b =
395 -56.021 mm for the longitudinal displacement in the abutment (Asia).
396

397 ## 5.2. Displacement at Bearing

398 The longitudinal and the vertical displacements of the tower bearings, P1 (Europe) and P2 (Asia),
399 are calculated. The longitudinal displacements at the bearings of the towers are shown in **Figure 16**.
400
401
402

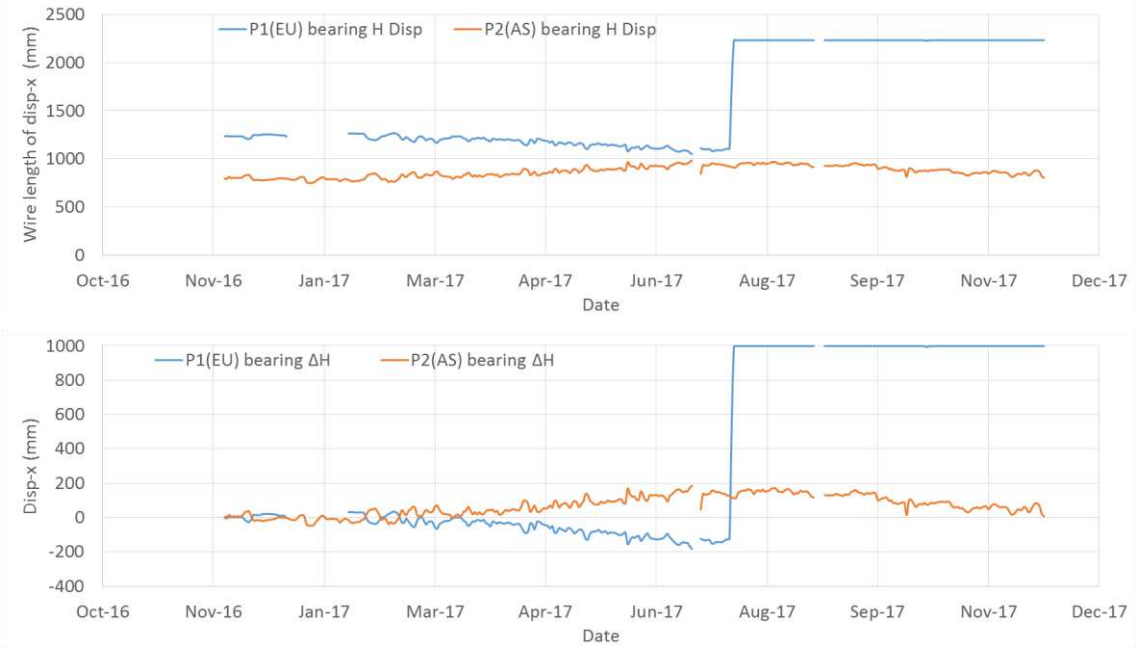


Figure 16 Daily average displacements at tower bearings in the longitudinal direction

However, the parts of them since August 2017 have unexpectedly jumped up to around 1 m, and indicating constantly 1 m with no change, so it seemed the horizontal displacement sensor would have a problem.

At the tower, P2 (Asia), the displacements in the longitudinal direction differ from ones at P1 (Europe). They are increasing along with the seasonal transition from the winter to the summer, which is attributed to the horizontal displacement sensor having a problem.

Since the range of displacements at P2 (Asia) is almost the same as at P1 (Europe), it seems there is a plus-minus sign error in the output values of the longitudinal displacements at P2 (Asia).

The vertical displacements (z) at the bearings of the towers, P1 and P2, are shown in **Figure 17**.

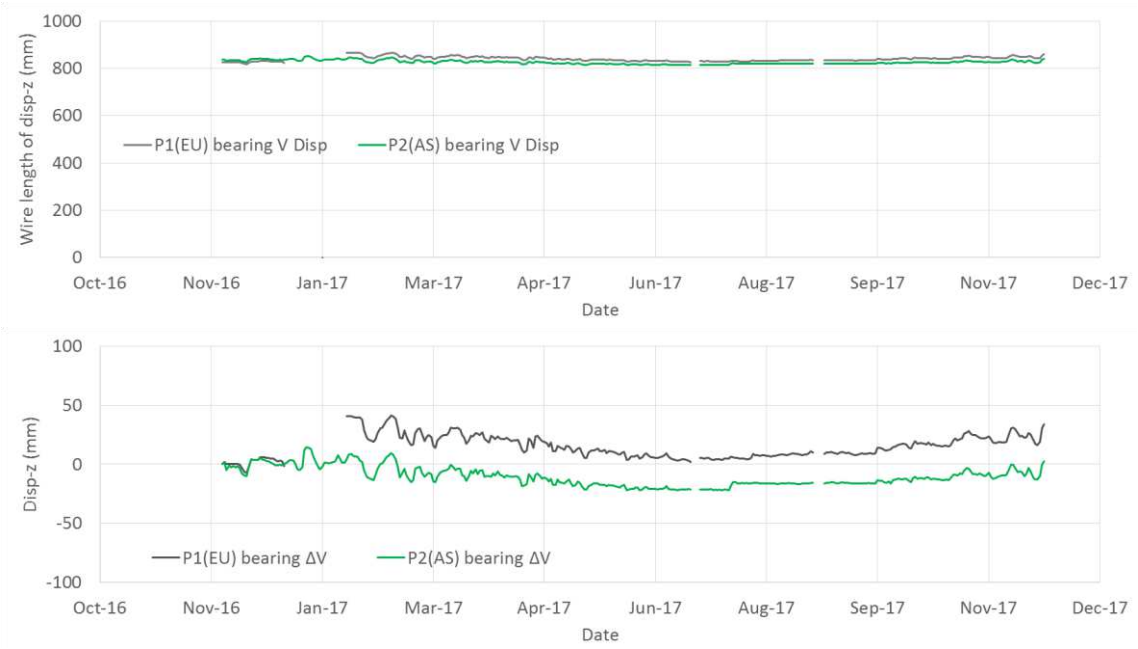


Figure 17 Daily average displacement at tower bearing in the vertical direction

The displacements calculated in the vertical direction (*z*-axis) are less correlated with the seasonal variation, compared to the displacements calculated in the longitudinal direction (*x*-axis).

As similar as described in the bridge abutments, the vertical displacements respond to the longitudinal displacements. Hence, it may be difficult to evaluate accurately the amount of the vertical displacements data alone.

The daily average longitudinal displacements of the tower bearings are plotted with respect to the deck effective temperature for exploring the temperature-displacement relationship, as shown in **Figure 18**.

It is noted that the output values of the longitudinal displacements at P2 have plus/minus switched, assumed that there is a plus-minus sign error.

Data segments exhibiting constant or non-physical values were excluded from regression analysis. Only displacement records showing continuous variation consistent with temperature changes were retained for evaluating temperature–displacement relationships.

As similar as described in the bridge abutment, the daily longitudinal displacements present a very good linear relationship with the deck effective temperature.

For P2, the maximum measured value was 185 mm, comparable to the corresponding analytical displacement range obtained from the design-stage numerical analysis.

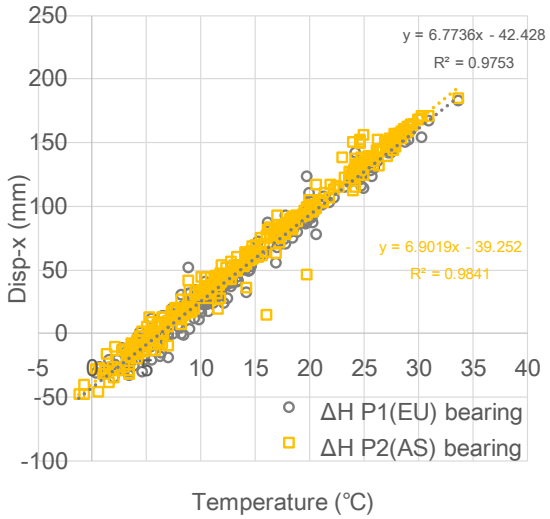


Figure 18 Relationship between daily average longitudinal displacement at tower bearing and deck effective temperature

The corresponding linear regression model is taken as

$$y = at + b + \varepsilon_y \quad [6]$$

where y is the displacement, a (slope) and b (intercept) are regression coefficients, and ε_y is the error. With least-square fitting, the regression coefficients are obtained as a = 6.773 mm/°C and b = -42.428 mm for the longitudinal displacement at P1 (Europe), and a = 6.902 mm/°C and b = -39.252 mm for the longitudinal displacement at P2 (Asia).

The regression coefficients for the displacement at other locations, not shown here for brevity, can be used to quantify the temperature-induced movement of the bridge.

Slope a is 9.253, 9.285, 6.773, and 6.902 mm/°C for the longitudinal displacements at the four displacement sensors (the European- and the Asian-side abutments and tower bearings) respectively.

The difference of the slope might be attributed to the distance from the middle of the bridge, while the thermal coefficients of linear expansion of steel and concrete are 1.2 and 1.0×10^{-5} / °C in the Eurocode 1. Thus, the global responses of the bridge are associated with the temperatures over the entire section.

5.3. Displacement of Bridge Deck

The bridge deck tends to move slightly in all directions, possibly because displacements are affected not only by temperature loading but also by other loadings such as traffic and wind. However, these effects are not isolated in the present study, and the analysis focuses on displacement components exhibiting consistent correlation with temperature.

The daily average displacements of bridge deck in mid-span are illustrated in **Figure 19**. A constant seasonal variation in the vertical displacements can be observed from the figure, including some influence from instant vehicle loading. In particular, the bridge deck moves downwards in the summer, and upwards in the winter. The vertical displacements (z-axis) are going down to around 500 mm at maximum in the summer period.

The longitudinal and the transverse displacements, however, do not exhibit a clear or stable seasonal correlation with temperature. They are showing in part the constant variation, but it seems hard to find the relationship of them with the seasonal trends. And they differ in the North and the South and even have an offset each other. The first part of the plot has sudden variations around March, and the transverse displacement values are much drifting. This error might be attributed to sensor accuracy and the initial value setting. And noise measurement is also another factor, so recalibration must be needed.

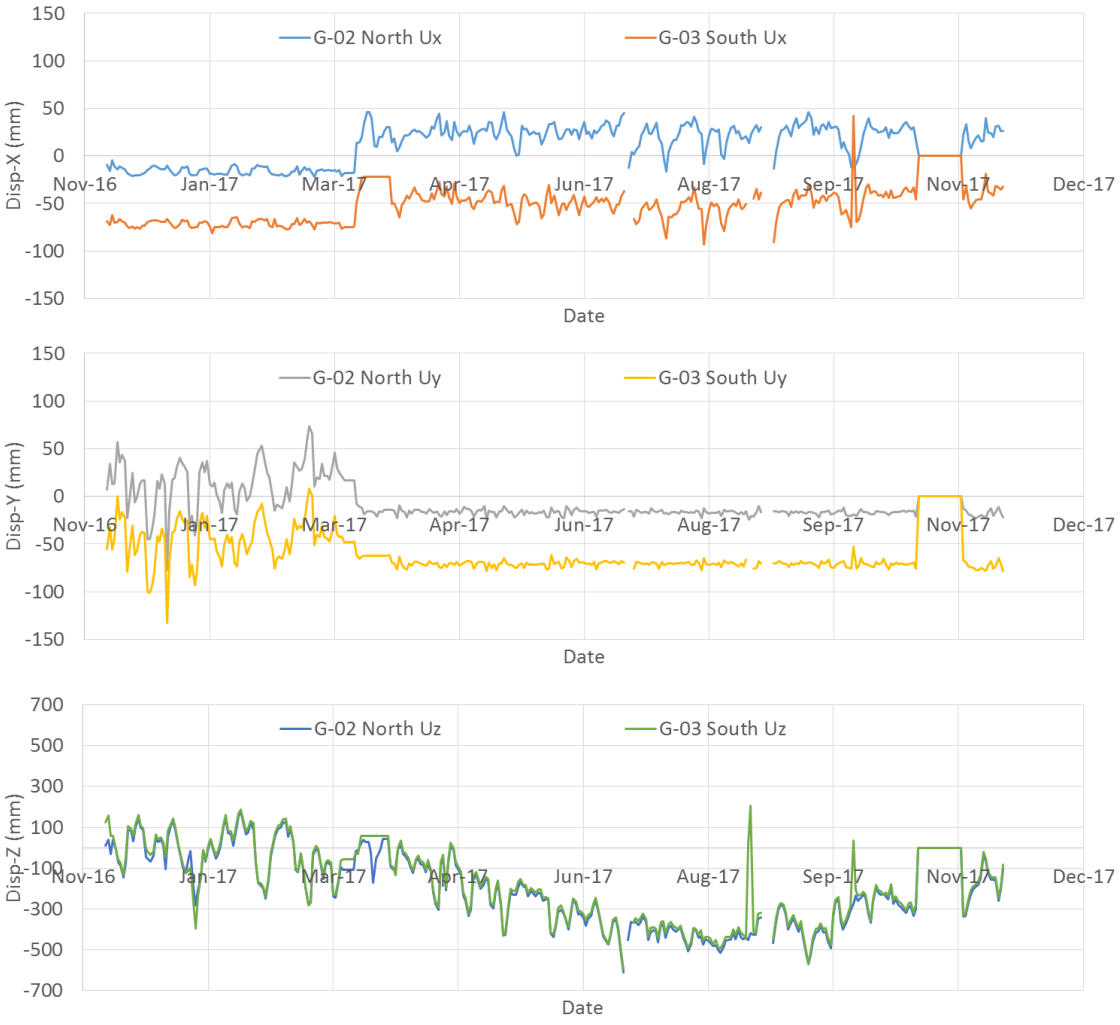


Figure 19 Daily average displacements of bridge deck in the middle of the main span (D28 block)

The daily average displacements for a year are also plotted with respect to the deck effective temperature for exploring the temperature-displacement relationship, as shown in **Figure 20**.

As found above, both longitudinal and transverse displacements turned out to have no clear relation with the temperature and then are excluded from displacement evaluation here.

The daily vertical displacements present a very good linear relationship with the seasonal variation. With respect to the deck effective temperature, the corresponding linear regression model is taken as

$$y = at + b + \varepsilon_y \quad [7]$$

where y is the displacement, a (slope) and b (intercept) are regression coefficients, and ε_y is the error. With least-square fitting, the regression coefficients are obtained as a = -19. 683 mm/℃ and b = 116.45 mm for the vertical displacement in the North, and a = -19. 321 mm/℃ and b = 129.35 mm for the vertical displacement in the South.

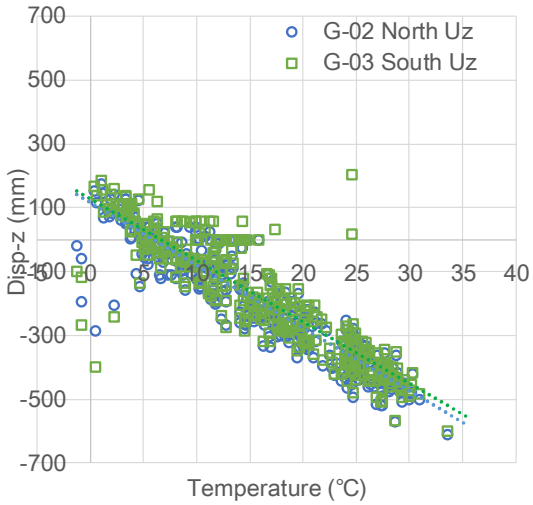


Figure 20 Relationship between daily average displacement of bridge deck (D28) and deck effective temperature during 2017

These field measurements demonstrate that temperature-induced displacement dominates the long-term deformation behavior of the bridge, with consistent linear relationships observed at multiple structural locations, providing a reliable empirical basis for thermal response interpretation.

The maximum difference of displacement (z-axis) reaches up to approximately 600 mm depending on the seasonal temperature change, and the measured maximum displacement is of the same order of magnitude as the analytical prediction (744 mm), while remaining within the expected design-stage envelope.

6. Conclusion

This study provides one of the first long-term, field-based characterizations of temperature-induced displacement in a hybrid cable-stayed and suspension bridge, based on a continuous one-year monitoring dataset. Unlike previous studies that focused primarily on short-term or diurnal thermal effects, the present work captures seasonal trends and cumulative thermal behavior, enabling direct observation of how thermal actions govern global bridge movements over time.

The results demonstrate that longitudinal displacements at abutments and tower bearings exhibit a strong and stable linear relationship with effective deck temperature, with seasonal movements reaching approximately 200 mm. Importantly, the analysis reveals that vertical displacements measured at these locations are predominantly secondary responses induced by longitudinal expansion and contraction, rather than direct effects of temperature variation alone. This finding provides a mechanistic interpretation of displacement sensor data and highlights the need for coupled evaluation of longitudinal and vertical measurements in long-span bridge monitoring.

At midspan, the bridge deck shows a clear and repeatable linear correlation between seasonal temperature variation and vertical displacement, with measured movements approaching 500 mm during summer periods. These observations offer a data-driven basis for defining displacement threshold levels under normal thermal conditions, supporting more reliable differentiation between temperature-induced behavior and abnormal structural response.

In addition, the long-term monitoring data enabled identification of sensor drift, sign inconsistency, and calibration issues that would not be detectable from short-duration measurements. This emphasizes the value of sustained monitoring not only for structural assessment but also for validating the reliability of SHM systems themselves.

Overall, the study advances the understanding of thermal effects on hybrid long-span bridges by linking long-term temperature measurements, structural response mechanisms, and monitoring system performance. The findings contribute to improved interpretation of SHM data and provide practical guidance for both bridge design verification and in-service performance evaluation under thermal actions.

7. Reference

[1] Operation and Maintenance Manual of Yavuz Sultan Selim Bridge, 2017

[2] You-Lin Xu, Yong Xia, Structural Health Monitoring of Long-Span Suspension Bridges, Spon Press, 2012

[3] Lan Chen, Fengwu Li, Linren Zhou, Jing Ji, Numerical simulation of wind effects on the temperature analysis of bridges, Porc. SPIE 9805, Health Monitoring of Structural and Biological Systems 2016, April 2016

537 [4] Linren Zhou, Yong Xia, Jame M. W. Brownjohn, Ki Young Koo, Temperature Analysis of a Long-
538 Span Suspension Bridge Based on Field Monitoring and Numerical Simulation, J. Bridge Eng.,
539 2016, 21(1)
540 [5] Yong Xia, Bo Chen, Xiao-qing Zhou, You-lin Xu, Field monitoring and numerical analysis of
541 Tsing Ma Suspension Bridge temperature behavior, Structural Control Health Monitoring, 2012
542 [6] Eurocode 1, Actions on bridges, Part 1-5 Thermal actions, EN1991-1-5
543 [7] Jean-Michel Lucas, Michel Virlogeux, Caude Louis, Temperature in the Box Girder of the
544 Normandy Bridge, Structural Engineering International, Vol. 15, No. 3, August 2005
545 [8] Elbadary, M.M., Ghali A., Temperature variations in concrete bridges, J. Structural Eng., 1983
546 [9] S. Topcu, S. Dilmac, and Z. Aslan, Study of hourly solar radiation data in Istanbul, Renewable
547 Energy, Vol.6, No.2, pp.171-174, 1995
548 [10] Analysis results – Service life – Static analysis control, Design report, 3rd Bosphorus Bridge,
549 2014
550 [11] Shashi Moorty, Charles W. Roeder, Temperature-Dependent Bridge Movements, Journal of
551 Structural Engineering, 118(4), 1090-1105, 1992
552
553